The Astrophysical Journal, 583:765–775, 2003 February 1

STELLAR HALO PARAMETERS FROM 4588 SUBDWARFS

Andrew Gould
Department of Astronomy, Ohio State University, 140 West 18th Avenue, Columbus, OH 43210;
gould@astronomy.ohio-state.edu
Received 2002 July 31; accepted 2002 October 8

ABSTRACT

Using a reduced proper-motion discriminator, I obtain a sample of 4588 subdwarfs from the revised New Luytens Two-Tenths (NLTT) Catalog of Salim & Gould. The ample statistics and low contamination permit much more precise determinations of halo parameters than has previously been possible. The stellar halo is not moving with respect to the local standard of rest (LSR) in either the vertical or radial direction, up to uncertainties of 2 km s^{-1}. This indicates that either the LSR is on a circular orbit or the Sun happens to lie very close to an extremum of the LSR's elliptical orbit. Similarly, tentative detections of vertical proper motion of Sgr A* relative to the LSR are either incorrect or they reflect real physical motion of the central black hole relative to the Galactic potential. The correlation coefficients of the halo velocity ellipsoid, which would reflect any possible misalignment between its principal axes and the cardinal directions of the Galaxy, vanish to within 2%. The halo subdwarf luminosity function peaks at $M_V \sim 10.5$ with an FWHM of about 2.5 mag.

Subject headings: Galaxy: halo — stars: kinematics — stars: luminosity function, mass function — stars: statistics — subdwarfs

1. INTRODUCTION

Samples of nearby halo stars can be analyzed to find the bulk properties of the population: their velocity, spatial, and metallicity distributions, as well as their luminosity function (LF). The principal difficulty is obtaining a sample that is large enough to draw statistically significant conclusions while still not being contaminated with disk and thick disk stars, which locally outnumber halo stars by a factor of $\sim 10^3$.

The most secure method to construct such a sample would be to obtain parallaxes, proper motions, and radial velocities (RVs) for a larger, unbiased sample of stars and then select halo stars based on their space motions. The *GAIA* satellite would be able to do this, but even under the most optimistic projections, its data will not be available for well over a decade.

In the absence of such ideal data sets, most nearby halo samples have been culled from catalogs of high proper-motion stars (although there are a few notable exceptions to this rule). For example, Dahn et al. (1995) obtained trigonometric parallaxes for about 100 proper-motion–selected stars, thereby determining their transverse velocities, distances, and absolute magnitudes. By rigorous selection on transverse velocity ($v_\perp > 260$ km s^{-1}), they obtained a sample that was virtually free of disk and thick-disk contamination. The distances and absolute magnitudes then allowed them to measure the LF. Of course, to do so they had to correct for the halo stars that were eliminated from their sample (along with the unwanted disk stars) by their stringent velocity criterion, and this in turn required a model of the halo velocity distribution.

The best such model up to that date was constructed by Casertano, Ratnatunga, & Bahcall (1990), who used maximum likelihood (ML) to decompose two proper-motion–selected samples into disk, thick disk, and halo components making use of both photometric and proper-motion data. They thereby identified different populations within the data, even though individual stars could not generally be unambiguously associated with a specific population. In particular, Casertano et al. (1990) showed that the likelihood fit was significantly improved by allowing for a third "intermediate" or thick disk population rather than just two. The kinematics of the halo when so fitted were more extreme than in the two-component fit earlier obtained by Bahcall & Casertano (1986) because thick-disk contamination was drastically reduced.

RR Lyrae stars are halo tracers selected on variability rather than proper motion. Estimates of the RR Lyrae absolute magnitude from statistical parallax automatically yield the velocity ellipsoid. While this technique has been applied for almost a century, only in the last decade or so has it been realized that the RR Lyrae samples are actually mixtures of thick-disk and halo stars. Since statistical parallax uses both RVs (whose spectra also yield metallicity information) and proper motions, and since it derives distances for all stars, full kinematic as well as metallicity information is generally available. In a series of papers, Layden (1994, 1995, 1997) both systematized preexisting data and obtained substantial new data, thereby laying the basis for a new statistical parallax solution that clearly separated the thick-disk and halo populations using a combination of kinematic and metallicity criteria (Layden et al. 1996). Popowski & Gould (1998a, 1998b) and Gould & Popowski (1998, collectively PG3) introduced new mathematical methods and on this basis conducted a thorough overhaul of the Layden et al. (1996) sample, recalibrating much of the old photographic photometry, incorporating more modern extinctions, identifying suspicious astrometry, and developing a new method to incorporate non–RR-Lyrae RVs into the analysis.

Of particular note in the present context, PG3 were the first to measure five of the nine components of the halo velocity ellipsoid: all previous analyses had measured the three diagonal components of the velocity dispersion tensor and the component of bulk motion in the tangential

direction (the asymmetric drift), but had assumed that the off-diagonal components as well as the bulk motion in the radial and vertical directions were zero. While the PG3 measurements all turned out to be consistent with zero (in the frame of the local standard of rest [LSR]), the error bars were tantalizingly close to being able to probe some interesting scientific questions.

The bulk motion of the halo in the radial and vertical directions is more likely to coincide with the rest frame of the Galaxy than is the motion of the LSR. The LSR could well be on an elliptical orbit, in which case it would be moving toward or away from the Galactic center unless the Sun happened to lie at an extremum of this orbit. Indeed, Blitz & Spergel (1991) claimed that the LSR is moving outward at 14 km s^{-1} based on radial-velocity measurements of gas in the outer Galaxy (assumed to be on circular orbits). On the other hand, Metzger & Schechter (1994) concluded that the LSR was moving inward at 6.6 ± 1.7 km s^{-1} based on RVs of carbon stars in the outer Galaxy.

Similarly, if the Milky Way disk is warped, then one would expect the LSR to be moving either up or down relative to the Galactic rest frame, unless the Sun happened to be at an extremum of the warp. Backer & Sramek (1999) found that Sgr A* is moving down at 17 ± 6 km s^{-1} relative to the LSR. If the supermassive black hole associated with Sgr A* is assumed to be at rest with respect to the Galaxy, then this apparent motion would actually be a reflex of the warped motion of the LSR. On the other hand, Reid et al. (1999) find that Sgr A* is moving in the opposite direction (although with much larger errors) at 15 ± 11 km s^{-1}. New more precise measurements are expected soon (M. Reid 2001, private communication).

For a roughly isotropic ensemble of N_s stars, the bulk motion U_i can be measured with a precision,

$$\sigma(U_i) \sim \sqrt{\frac{3\ c_{ii}}{n_d N_s}}\,, \tag{1}$$

where c_{ii} is the dispersion in the ith direction and n_d is the number of components of the velocity measured for each star. For the PG3 sample, $N_s \sim 170$ and $n_d = 3$, while $c_{11} \sim (160 \text{ km s}^{-1})^2$ and $c_{33} \sim (90 \text{ km s}^{-1})^2$. Hence, $\sigma(U_1) \sim 13$ km s^{-1} and $\sigma(U_3) \sim 8$ km s^{-1}. Therefore, the PG3 measurement errors were not quite small enough to probe these interesting questions.

Of course, measurement of a difference between the bulk-halo and LSR velocities would not be unambiguous evidence of LSR motion (Oresme 1377). For example, the angular momentum vector of material infalling onto the Milky Way could have radically changed between the time of the formation of the halo and disk. Therefore, the former could, in principle, be rotating in a basically polar orbit (albeit with low Mach number) relative to the latter. Hence, any sort of relative motion would be intriguing evidence of a nonsimple Galaxy whose exact origins would have to be sorted out making use of other data and arguments.

Similarly, the off-diagonal elements of the velocity dispersion tensor (normalized to the diagonal elements) $\tilde{c}_{ij}$ could potentially provide evidence of asymmetries of the Galaxy that would reflect on its origins. The errors in these quantities are $\sim(n_d N_s/3)^{-1/2}$, or about 8% for the RR Lyrae sample. To the best of my knowledge, no one has investigated what might cause these quantities to differ from zero, so I do not know whether their consistency with zero at the 8% level challenges or confirms any theory. Nevertheless, it seems interesting to try to probe the off-diagonal elements at higher precision.

The status of the LF and local density of the stellar halo are also somewhat controversial. Dahn et al. (1995) find that the LF peaks at around $M_V \sim 12$, in qualitative agreement with the shape of the LF seen in undisturbed globular clusters (Piotto, Cool, & King 1997). However, Bahcall & Casertano (1986) and Gould, Flynn, & Bahcall (1998) find a roughly flat LF over the interval $9 \lesssim M_V \lesssim 13$. While Dahn et al. (1995) and Bahcall & Casertano (1986) both studied local stars drawn from proper-motion catalogs, Gould et al. (1998) adopted a radically different approach: they located stars in *Hubble Space Telescope* images that were too faint at their observed color to be in the disk and so were assigned absolute magnitudes and distances based on a halo color-magnitude relation. These stars were generally quite distant ($\gtrsim 3$ kpc) and therefore perhaps not directly comparable to the local samples. Sommer-Larsen & Zhen (1990) had earlier suggested that the stellar halo actually has two components, one roughly spheroidal and one highly flattened. (The highly flattened component is not to be confused with the thick disk: it is not rotating significantly.) In their model, the two components have roughly equal densities at the solar circle. Such a model predicts that the halo density should be roughly twice as great in the solar neighborhood as it is at a similar Galactocentric radius but a few kpc above the Galactic plane. Indeed, Gould et al. (1998) found a halo density that was lower than the Dahn et al. (1995) measurements by just this fraction. Recently, Siegel et al. (2002) have argued on the basis of a sample of 70,000 stars along multiple pencil beams that even a two-component halo model is inadequate to explain their star counts.

The newly released revised New Luytens Two-Tenths (NLTT) Catalog (Gould & Salim 2003; Salim & Gould 2003) allows one to obtain a very large and very clean sample of halo stars. The reduced proper-motion (RPM) diagram using the newly obtained $V-J$ colors clearly separates main-sequence stars, subdwarfs, and white dwarfs into different tracks (Salim & Gould 2002) in sharp contrast to the RPM diagram constructed from the original NLTT (Luyten 1979a, 1980). Although the first release of this catalog covers only 44% of the sky, it contains more than 5000 local halo stars, over an order of magnitude more than have ever been cleanly distinguished from disk stars on a star-by-star basis. This sample therefore opens the way to a much more detailed study of the local halo population than has previously been possible. In its present form, the sample does have some limitations. Since most of its stars lack RVs and parallaxes, it is not possible to establish the absolute distances or the amplitude of the velocity ellipsoid based on the revised NLTT catalog alone. Nevertheless, the amplitude of the velocity ellipsoid is already known with a precision of about 10% from previous studies, and by incorporating this external information one can obtain much more precise measurements of the five components of the ellipsoid that are currently poorly measured: U_1, U_3, and $\tilde{c}_{ij}$. Once the velocity scale is set, the mean distances to the stars are also determined, which permits one to measure the LF. The large number of stars in the sample therefore offers the hope of probing the bottom of the subdwarf sequence, which, because of its dimness, is poorly represented in magnitude-limited samples. Finally, the catalog contains a large

number of stars from the Galactic plane to about $z \sim \bar{V}_\perp/\mu_{\rm lim} \sim 350$ pc above the plane, where $\bar{V}_\perp \sim 300$ km s^{-1} is the typical transverse speed seen toward the Galactic poles and $\mu_{\rm lim} = 180$ mas yr^{-1} is the proper-motion limit of the catalog. While this distance is short compared to the several kiloparsecs hypothesized as the height of the flattened halo component, the large number of stars in the sample may yield a statistically significant statement about the presence of a density gradient on these larger scales.

ML analysis is absolutely critical for extracting halo parameters from this catalog. For example, since the mean tangential velocity of stars seen toward the Galactic poles is $\sim$200 km s^{-1}, one might naively expect that the stars selected toward the poles would have, on average, this velocity. However, given the fact that the sample is proper-motion limited, for all but the dimmest absolute magnitudes the number of stars seen with velocities that are 1 σ higher than average (300 km s^{-1}) is $(300/100)^3 = 27$ times higher than the number with velocities that are 1 σ lower (100 km s^{-1}). This severe selection bias does not *directly* affect any other parameters. However, it couples through the highly uneven (but perfectly known) sky coverage from Two Micron All Sky Survey (2MASS) to *indirectly* affect essentially all other parameters. These effects can only be removed by comparing the predictions of models with the observations, as ML does automatically.

Hence, I begin in § 2 by giving a careful summary of the ML modeling procedure. In § 3, I present my results and comment on various aspects of these whose interpretation requires caution. Finally, in § 4, I compare my results to previous work and briefly discuss the implications of this comparison. I reserve to the Appendix a somewhat technical discussion of the problems in determining the completeness of the revised NLTT catalog and the impact of this completeness on parameter estimation.

2. MAXIMUM LIKELIHOOD FORMULATION

2.1. *General Equation*

I use ML to estimate the parameters of the stellar halo. In general, a given data set is described by m observables $z_{{\rm obs},i}$, which I collectively denote $z^m_{\rm obs}$. If this m-dimensional space of observables is divided into bins of volume $\prod_{i=1}^m \Delta z_{{\rm obs},i}$, then the likelihood of detecting n_k objects in the kth bin is $L_k = \tau_k^{n_k} \exp(-\tau_k)/n_k!$, where $\tau_k = P_k(z^m_{\rm obs}) \prod_{i=1}^m \Delta z_{{\rm obs},i}$, and P_k is the probability density predicted by a given model. If the bins are now made sufficiently small that $\tau_k \ll 1$, then $n_k \leq 1$ and hence $n_k! = 1$. The logarithm of the product of the likelihoods from all the bins is therefore

$$\ln L = \sum_k \ln L_k = \sum_k n_k \ln \tau_k - \sum_k \tau_k \ . \tag{2}$$

The last term is just the total number of detections expected in the model, $N_{\rm exp}$. Since the n_k in the first term are either 0 or 1, equation (2) can be rewritten

$$\ln L = \sum_{k=1}^{N_{\rm det}} \ln[P_k(z^m_{\rm obs}) \prod_{i=1}^m \Delta z_{{\rm obs},i}] - N_{\rm exp} \ , \tag{3}$$

where $N_{\rm det}$ is the total number of detections. In general, however, the probability density is not most naturally written directly as a function of the observables $z_{{\rm obs},i}$ but rather of the model coordinates, $z_{{\rm mod},i}$, which are evaluated at the observables. Equation (3) can be rewritten in terms of these,

$$\ln L = \sum_{k=1}^{N_{\rm det}} \ln\{P_k[z^m(z^m_{\rm obs})]\mathcal{J}\} - N_{\rm exp} + N_{\rm det} \sum_{i=1}^m \ln \Delta z_{{\rm obs},i} \ , \tag{4}$$

where $\mathcal{J}$ is the Jacobian of the transformation from the observables to the model coordinates. For a given set of observations, the last term is the same for all models and so can be dropped.

2.2. *Jacobian*

In the present case, for each star there are six observables: the angular position on the sky $(l,\ b)$, the proper motion $(\mu_l,\ \mu_b)$, and the two photometric magnitudes $(V,\ J)$. There are also six model coordinates: the three spatial coordinates $\boldsymbol{r}$, the two components of transverse velocity $\boldsymbol{v}_\perp$, and the absolute magnitude, M_V. Hence,

$$\mathcal{J} = \left| \frac{\partial(\boldsymbol{r},\ \boldsymbol{v}_\perp,\ M_V)}{\partial(l,\ b,\ \mu_l,\ \mu_b,\ V,\ J)} \right| = r^4 \cos b \left| \frac{\partial(r,\ M_V)}{\partial(V,\ J)} \right| . \tag{5}$$

To evaluate $\mathcal{J}$, I write r and M_V as implicit functions of V and J, making use of the color-magnitude relation, $M_V = F[(V-J)_0]$,

$$r = 10^{0.2[V - A_V(r) - M_V]+1}, \quad M_V = F\left[V - J - \frac{A_V(r)}{R_{VJ}} \right] . \tag{6}$$

Here $A_V(r)$ is the extinction along the line of sight and $R_{VJ} \equiv A_V/E(V-J) = 1.38$ is the ratio of total to selective extinction. Partial differentiation of equation (6) yields the matrix equation

$$\begin{pmatrix} r & \dfrac{5}{\ln 10} + A'r \\ 1 & \dfrac{F'A'}{R_{VJ}} \end{pmatrix} \begin{pmatrix} \dfrac{\partial r}{\partial V} & \dfrac{\partial r}{\partial J} \\ \dfrac{\partial M_V}{\partial V} & \dfrac{\partial M_V}{\partial J} \end{pmatrix} = \begin{pmatrix} r & 0 \\ F' & -F' \end{pmatrix} \tag{7}$$

whose determinant gives,

$$\mathcal{J} = \frac{\ln 10}{5} \cos b\, r^5 F' Q,$$
$$Q \equiv \left| 1 - \frac{\ln 10}{5} \frac{dA_V}{d \ln r} \left(\frac{F'}{R_{VJ}} - 1 \right) \right|^{-1} . \tag{8}$$

If the reddening vector were parallel to the subdwarf sequence ($F'/R_{VJ} \simeq 1$), then the additional term Q in equation (8) would be negligible. In fact, however, this ratio is roughly $F'/R_{VJ} \sim 2.6$, which means that at typical distances $r \sim 300$ pc and low Galactic latitudes, $\ln Q \sim 0.12$, and so it cannot be ignored. Note that the prefactor $(0.2 \ln 10 \cos b)$ is an irrelevant constant and can be dropped in practical calculations, so that $\mathcal{J} \rightarrow r^5 F' Q$.

2.3. *Model Parameters*

I model the stellar halo distribution as the product of an LF, a velocity distribution, and a density profile. In addition, halo stars are assumed to obey a linear color-magnitude relation

$$M_V = F[(V-J)_0] = a(V-J)_0 + b \ . \tag{9}$$

In principle, one might also assume that this relation has

some intrinsic dispersion. However, for reasons that I discuss below, I do not include such a parameter in the model. Finally, not all halo stars satisfying the selection criteria will be detected. I therefore include in the model two parameters $(V_{\rm break},\ f_{\rm break})$ that describe the completeness as a function of apparent V magnitude,

$$C(V) = 1 \quad (V < 12)\ ,$$
$$C(V) = \frac{(V_{\rm break} - V) + f_{\rm break}(V - 12)}{(V_{\rm break} - 12)} \quad (12 < V < V_{\rm break})\ ,$$
$$C(V) = \frac{f_{\rm break}(20 - V_{\rm break}) + (V - V_{\rm break})}{(20 - V_{\rm break})} \quad (V_{\rm break} < V < 20)\ . \quad (10)$$

This form is motivated by the fact that NLTT is known to be complete to at least $V = 11$ away from the plane, and the revised NLTT catalog has captured essentially all of these stars (Gould & Salim 2003). The completeness falls precipitously at faint magnitudes, $V \gtrsim 18$. The simplest hypothesis is that it is linear over the intervening magnitudes.

I model the LF with 13 free parameters, one for each magnitude bin centered at $M_V = 3$–15. I model the velocity distribution as a Gaussian ellipsoid with nine parameters: three for the bulk motion U_i, three for the diagonal components of the dispersion tensor c_{ii}, and three for the off-diagonal components $c_{ij} (i < j)$. In practice, I use the normalized components of the latter (the correlation coefficients) $\tilde{c}_{ij} = c_{ij}/(c_{ii}c_{jj})^{1/2}$. It is known that the halo velocity distribution is highly non-Gaussian, with a kurtosis that is higher than Gaussian in the vertical direction, lower than Gaussian in the radial direction, and roughly Gaussian in the direction of rotation (PG3). However, modeling the non-Gaussian character of the distribution would be quite complicated, and it is straightforward to show that a ML fit of a non-Gaussian distribution to a Gaussian model returns unbiased estimates of the first two moments. Hence, there is no benefit to modeling the non-Gaussian form of the distribution unless one wants to investigate the higher moments of the distribution. Since these are not a focus of interest in the current paper, I opt for the simpler Gaussian model.

I model the halo distribution as falling as a power law with Galactocentric distance R and exponentially with distance from the Galactic plane z, i.e., $\rho = \rho_0 (R/R_0)^{-\nu} \exp(-\kappa|z|)$. The spatial distribution is therefore described by two parameters, ν and κ, where κ may be regarded as the inverse scale height. I adopt $R_0 = 8$ kpc.

Hence, I begin with 28 free parameters, 13 for the LF, nine for the velocity ellipsoid, two for the color-magnitude relation, two for the completeness function, and two for the density profile. However, as I now explain, there is one almost perfect degeneracy among these parameters, and therefore one of them must be fixed. If the zero-point b of the color-magnitude relation (eq. [9]) is increased by Δb, and all the bulk velocities U_i and dispersions $(c_{ii})^{1/2}$ are reduced by $10^{-0.2\Delta b}$, then all of the model's predicted proper motions will remain unchanged. The only difference will be that a star's absolute magnitude (inferred from its color) will be increased by $\Delta M_V = \Delta b$, and so the inferred density of stars of each resulting magnitude bin will be increased by $10^{0.6\Delta b}$. Actually, this scaling remains perfect only in the limit $A_V \to 0$, but since the extinction is quite small, the degeneracy is almost perfect.

I therefore fix

$$U_2 = -216.6 \text{ km s}^{-1}\ , \quad (11)$$

the value measured by Gould & Popowski (1998) for their "kinematically selected" sample of halo RR Lyrae stars. Gould & Popowski (1998) also evaluated the velocity ellipsoid for a "non-kinematically selected" sample of halo stars, with $U_2 = -198 \pm 9$ km s^{-1} somewhat less extreme than given by equation (11). Similarly, the non-kinematically selected sample of Norris (1986) gives $U_2 = -183 \pm 10$ km s^{-1}. However, as I describe in § 2.5 below, the present sample is effectively selected using a combination of kinematic and metallicity criteria, just as was true for the Gould & Popowski (1998) "kinematically selected" sample. Therefore, the scale of the velocity ellipsoid should be fixed by the "kinematically selected" rather than the Gould & Popowski (1998) "non-kinematically selected" sample.

Finally, as noted above, I do not include a parameter for the dispersion in the color-magnitude relation despite the fact that the halo is known to contain a range of metallicities and, therefore, a range of absolute magnitudes at fixed color and hence some dispersion $\sigma(M_V)$. Since I do not include this term, the velocity dispersions found by the ML fit will be larger than the true dispersions by

$$\Delta c_{ii} = (U_i^2 + c_{ii})[0.2 \ln 10 \sigma(M_V)]^2\ . \quad (12)$$

Hence, in principle, if one knew the c_{ii} sufficiently well, one could fix them (or one of them or their sum), and fit for $\sigma(M_V)$. However, as I show in § 3, the differences Δc_{ii} are smaller than the present uncertainties in the c_{ii}, and therefore this is not a practical possibility. Thus, the fit parameters that I am calling "c_{ii}" are actually shorthand labels for $c_{ii} + \Delta c_{ii}$. This means that the derived parameters will not yield new determinations for the c_{ii}. The best one can do is use these measurements to place rough upper limits on $\sigma(M_V)$. That is, among the nine velocity-ellipsoid parameters U_i, c_{ii}, $\tilde{c}_{ij}$, new values will be obtained for only five: U_1, U_3, and $\tilde{c}_{ij}$.

2.4. *Data Characteristics*

Among the six observables $(l,\ b,\ \mu_l,\ \mu_b,\ V,\ J)$ only the V magnitude has significant errors. The angular coordinates $(l,\ b)$ are known to 130 mas, about 6 orders of magnitude smaller than the scale on which there are significant density gradients. The proper-motion errors are 5.5 mas yr^{-1} or 3% of the NLTT proper-motion threshold. Since the intrinsic dispersion in proper motions is of order unity, and since the measurement errors add in quadrature to these, these errors are utterly negligible. The V errors are about 0.25 mag (Salim & Gould 2000). As discussed by Salim & Gould (2003), these are multiplied by 2.1 when entering the RPM and therefore cannot be ignored. Finally, the J errors are typically 0.03 mag. Even though they enter the RPM with somewhat higher weight (3.1), they are then added in quadrature to the V errors, and so are also negligible.

The errors in the original NLTT proper motions were 20 mas yr^{-1} (Salim & Gould 2003). These proper motions are not used directly in the evaluation of the likelihood, but they do have an indirect effect because they influenced Luyten's determination of which stars met his proper-motion threshold of 180 mas yr^{-1} and thus which ones ultimately entered

the revised NLTT catalog (Gould & Salim 2003; Salim & Gould 2003).

2.5. *Selection Criteria*

One wishes to select as large a sample of halo stars as possible, while effectively excluding stars from other populations. Moreover, one would like to restrict selection to those areas of the sky with homogeneous completeness characteristics. To achieve the first goal, I make use of the discriminator η introduced by Salim & Gould (2003),

$$\eta(V_{\rm RPM},\ V-J,\ \sin b) = V_{\rm RPM} - 3.1(V-J) - 1.47|\sin b| - 2.73\ , \quad (13)$$

where $V_{\rm RPM} = V + 5\log(\mu)$ is the RPM. Using the (V, $V-J$) RPM diagram, Salim & Gould (2003) showed that stars in the range $0 < \eta < 5.15$ are mostly halo stars. To be conservative, I restrict the selection by an additional magnitude on each end and require $1 < \eta < 4.15$ (see Salim & Gould 2003, Fig. 3). Completeness of the original NLTT catalog deteriorates significantly in areas south of POSS I, and Salim & Gould (2003) did not even attempt to recover faint NLTT stars in this region because their method cannot be applied there. I therefore require $\delta > -32\fdg4$. Salim & Gould (2003) showed that in the Galactic latitude interval $-0.2 < \sin b < 0.3$, NLTT completeness of main-sequence stars is severely affected, dropping from neighboring zones at higher latitude by a factor of $\sim$10. While the effect is much smaller for subdwarfs (and perhaps negligible for white dwarfs), to be conservative I restrict selection to stars outside this range. Finally, of course, the identifications by Salim & Gould (2003) rely critically on 2MASS and so have only been carried out for the 47% of the sky (57% of the region $\delta > -32\fdg4$) that is covered by the second incremental 2MASS release. Hence, the spatial selection function alone is quite complex. This fact, together with the large number of observables, implies that great care is required to evaluate the likelihood function.

Note that the discriminator η (eq. [13]) is effectively a function of both kinematics and metallicity. That is, η increases both with higher transverse velocity and with lower metallicity (and so lower luminosity at fixed color). It is for this reason that I said in § 2.3 that the sample is selected using a combination of kinematic and metallicity criteria.

2.6. *Likelihood Evaluation*

In order to find the model parameters that maximize the likelihood, one must compare in a consistent way the likelihood of observing the data given different sets of model parameters. This statement is so obvious that it would appear not worth mentioning. However, achieving such consistency is by no means trivial.

The first term in equation (4) is relatively straightforward to calculate because it depends only on differential probability functions that are multiplied together. However, the second term, the total number of stars expected to enter the sample for a given model is quite complicated in several respects. First, as discussed in § 2.5 the selection criteria themselves are complex. Second, to estimate $N_{\rm exp}$ requires an integral over nine dimensions: six for the model coordinates ($\boldsymbol{r}$, $\boldsymbol{v}_\perp$, M_V), plus three for the measurement errors (V, $\mu_{l,\rm NLTT}$, $\mu_{b,\rm NLTT}$). Recall that even though I am not making use of the NLTT proper-motion measurements, they still enter the likelihood function because they affect the sample selection.

Integration over more than four dimensions is in general more efficiently carried out by Monte Carlo than directly. In the present case, the complexity of the 2MASS coverage further reinforces the advantages of Monte Carlo integration. However, such an approach poses significant difficulties when comparing likelihood estimates at different locations in parameter space: Monte Carlo integration introduces Poisson fluctuations into the evaluation of $N_{\rm exp}$, which are of order the square root of the size of the random sample. While these fluctuations can to some extent be suppressed by insisting that all realizations have the same sample size, the induced fluctuations remain of the same order. To be certain that these do not induce roughness in the ML surface of order unity would require Monte Carlo samples of $O(10^7)$, which would be computationally prohibitive.

To counter this problem, rather than directly assembling a separate catalog of fake stars for each model, I assemble a single catalog of fake stars and assign the stars different weights according to the model. That is, I first choose a baseline model that is reasonably close to the final model. For each magnitude bin, I assign an absolute magnitude drawn uniformly over this bin, a physical location drawn uniformly from the volume within 1 kpc of the Sun, and a transverse velocity drawn randomly from the two-dimensional Gaussian projected-velocity distribution expected in the baseline model. I note the Gaussian probability of each such fake star but do not at this point make use of it.

Next I determine the observational characteristics of the star. For example, I use the color-magnitude relation of the baseline model and the star's distance to obtain the true $(V-J)_0$ color and V_0 magnitude. I draw the error in the observed V magnitude from a Gaussian distribution and redden both the color and magnitude according to a simplified extinction law,

$$A_V(r,\ b) = 0.075\ |\csc b|[1 - \exp(-r\sin|b|/h_d)]\ , \quad (14)$$

where $h_d = 130$ pc is the dust scale height. Similarly, I obtain the true proper motion from the distance and transverse velocity and draw the two NLTT proper-motion errors from a Gaussian distribution. If the NLTT proper motion exceeds 180 mas yr^{-1}, and the RPM discriminator η lies within somewhat expanded bounds ($-1 < \eta < 6.15$) as calculated within the baseline model, I accept the star into a master list of fake stars. For each model I examine each star on this master list and recalculate ($V-J$) using the model's color-magnitude relation. I accept only stars satisfying the selection criterion ($1 < \eta < 4.15$) as calculated within the model. Next, I determine $N_{\rm exp}$ by counting all of the fake stars thus accepted and assigning each one a weight that depends on the model. The weight is a product of factors: $(R/R_0)^{-\nu}$ for proximity to the Galactic center, $\exp(-\kappa|z|)$ for distance from the Galactic plane, $C(V)$ to take account of completeness, as well as a factor for the luminosity function of the star's M_V bin. In particular, I evaluate the probability of the transverse velocity given the model and divide this by the tabulated probability of the baseline model. In this way, $N_{\rm exp}$ is evaluated stochastically for an ensemble of models, without introducing random noise into the *relative* values obtained for different models.

For purposes of finding the best-fit model, I use a catalog of fake stars drawn from a model that is 100 times denser than the actual stellar halo, so that the stochastic character of the fake catalog introduces errors in the parameter estimates that are 10 times smaller than the Poisson errors. I use the bootstrap method to calculate the errors in the parameters; i.e., I evaluate the scatter in model fits to 25 realizations of the data formed by drawing randomly from the actual data with replacement. Each realization is tested against the *same* catalog of fake data. For this purpose, I use a fake catalog drawn from a model that is 10 times denser than the actual stellar halo.

3. RESULTS

The best-fit model to the 4588 subdwarfs selected according to the criteria described in § 2.5 has the following characteristics.

3.1. *Velocity Ellipsoid Parameters*

For the bulk halo motion relative to the Sun, I find

$$U_1 = 11.4 \pm 2.2 \text{ km s}^{-1}\,, \qquad U_3 = -5.4 \pm 2.4 \text{ km s}^{-1}\,, \tag{15}$$

in the (outward) radial and (upward) vertical directions. Since the Sun moves relative to the LSR at -10.0 ± 0.4 km s^{-1} and 7.2 ± 0.4 km s^{-1} in these directions (Dehnen & Binney 1998), this implies that the LSR is moving relative to the halo at -1.4 ± 2.2 km s^{-1} radially and -1.8 ± 2.4 km s^{-1} vertically. That is, both components are consistent with zero. If the halo is assumed to be stationary in both directions relative to the Galactic potential, then either the deviations of the LSR from a circular orbit must be very small, or the Sun must lie close to the extrema of these deviations. On the other hand, if the halo is not stationary, then it just happens to have almost exactly the same motion as the LSR, which would be a most surprising coincidence.

The errors in equation (15) include only the statistical errors within the fit and not the systematic errors induced by fixing the amplitude of the velocity ellipsoid using the Gould & Popowski (1998) value for $U_2 = -216.6$ km s^{-1}. However, as I now show, this systematic error is relatively small. First, the statistical error of U_2 is 12.5 km s^{-1} or 6%. This induces a systematic error in U_1 also of 6%, that is, 0.7 km s^{-1}, which is small compared to the statistical error. There is a second source of error because, while both the present sample and the Gould & Popowski (1998) sample were chosen based on a combination of kinematic and metallicity criteria, those criteria are not identical nor even easily comparable. Hence, the values of U_2 for the two samples need not be identical. It is difficult to judge the size of this systematic error, but it is probably also of order 10 km s^{-1}, i.e., about 5%, and therefore again much smaller than the statistical error. The systematic errors scale with U_i and therefore are about half as big for the vertical motion as the radial motion.

The three off-diagonal components to the velocity-dispersion tensor are

$$\tilde{c}_{12} = 0.024 \pm 0.014\,, \qquad \tilde{c}_{13} = 0.005 \pm 0.023\,,$$
$$\tilde{c}_{23} = -0.004 \pm 0.026\,. \tag{16}$$

That is, all three are consistent with zero at about the 2% level. (Because there are five velocity-ellipsoid parameters being fitted, the 1.7 σ "detection" of $\tilde{c}_{12}$ cannot be regarded as even marginally significant.)

Finally, the three diagonal components are

$$\sqrt{c_{ii} + \Delta c_{ii}} = (162.4 \pm 1.4\,, \quad 105.8 \pm 1.7\,, \quad 89.4 \pm 1.9) \text{ km s}^{-1}\,, \tag{17}$$

where Δc_{ii} is defined by equation (12). This can be compared to values of c_{ii} found by Gould & Popowski (1998) for kinematically selected RR Lyrae stars.

$$\sqrt{c_{ii}} = (171 \pm 10\,, \quad 99 \pm 8\,, \quad 90 \pm 7) \text{ km s}^{-1}\,, \quad \text{(RR Lyraes)}\,. \tag{18}$$

If the errors in equation (18) were sufficient small, it would be possible to determine the Δc_{ii} in equation (17) and so characterize $\sigma(M_V)$ (the scatter in M_V at fixed $V-J$ color; see eq. [12]). However, given the errors, it is immediately clear that $\sigma(M_V)$ is consistent with zero. To find out what upper bound can be put on $\sigma(M_V)$, I first note that because $c_{22}/U_2^2 \sim 5$, most of the potential information comes from the tangential component. At the 1 σ level, $(\Delta c_{22})^{1/2} < 55$ km s^{-1}. Hence, from equation (12), $\sigma(M_V) < 0.5$. This is not a very interesting 1 σ limit. Moreover, I have not yet incorporated the statistical or systematic uncertainties in the amplitude of the velocity ellipsoid as discussed following equation (15). Hence, equations (17) and (18) present a reasonably consistent picture but do not significantly constrain $\sigma(M_V)$. I do note, however, that the comparison of these two equations shows that the choice for normalizing the velocity ellipsoid, $U_2 = -216.6$ km s^{-1}, cannot be off by more than about 15%. If it were, then the fitted values for $(c_{ii} + \Delta c_{ii})^{1/2}$ would also change by 15%, and these would then be inconsistent at high significance with the c_{11} and c_{33} as measured for RR Lyrae stars. For reference, the dispersions $(c_{ii})^{1/2}$ from the non-kinematically selected samples of Gould & Popowski (1998) and Norris (1986) are $(160 \pm 7,\ 109 \pm 8,\ 94 \pm 5)$ km s^{-1} and $(131 \pm 6,\ 106 \pm 6,\ 85 \pm 4)$ km s^{-1}, respectively.

3.2. *Halo Profile Parameters*

The halo density is not expected to vary much over the small ($\sim$300 pc) volume that is being probed. As discussed in § 2.3, I therefore model the density profile simply as $\rho = \rho_0 (R/R_0)^{-\nu} \exp(-\kappa|z|)$. I find

$$\nu = 3.1 \pm 1.0\,, \qquad \kappa = 0.022 \pm 0.057 \text{ kpc}^{-1}\,. \tag{19}$$

The estimate of ν is consistent with many previous determinations, which because they are measured over longer baselines, have much smaller errors. For example, Gould et al. (1998) find $\nu = 2.96 \pm 0.27$. The κ measurement is quite interesting despite the fact that (or rather precisely because) it is consistent with zero. At the 2 σ level, this constrains the scale height to be $\kappa^{-1} > 7$ kpc. If the local halo were composed of two components, one highly flattened and one roughly round, then one would expect the density to fall off locally over distances that are short compared 7 kpc. Hence, this result should help constrain two-component halo models.

3.3. *Color-Magnitude Relation*

I fit for a color-magnitude relation of the form $M_V = a(V-J)_0 + b$ (eq. [9]) and find

$$a = 3.59\ , \qquad b = 0.69\ . \tag{20}$$

The formal uncertainties on these parameters are very small, of order 0.01 mag. However, recall from the discussion above equation (11) that b is completely degenerate with the amplitude of the velocity ellipsoid, which was fixed for purposes of the fit but which actually has a statistical uncertainty of 6% (and a comparable systematic error). Hence, the true error in b is about 0.2 mag. The total error in a is probably not much larger than the formal error.

3.4. *Luminosity Function*

The LF is parameterized by 13 separate 1 mag bins, with centers from $M_V = 3$ to 15. I find (as did Gould, Bahcall, & Flynn 1997 when they studied the disk LF) that ML estimates of the LF tend to magnify Poisson fluctuations according to the following mechanism. First suppose that the true LF has a dip at a certain bin. Observational errors will scatter stars from the two neighboring bins into this bin, thus tending to wash out the dip. Hence, a ML fit, when confronted by a dip in the observed distribution will tend to accentuate it as it reconstructs the underlying (true) LF. Now suppose that the true LF is flat over three adjacent bins but because of Poisson fluctuations the central bin is depressed. ML will also accentuate this dip in an attempt to reconstruct the "true" LF. Hence, particularly for bins with low total counts, ML can introduce structure that is not really present. I handle this potential problem by imposing a "roughness" penalty $\Delta L = 16$ (difference/sum)^2, where "sum" and "difference" refer to the sum and difference of the LF in each pair of neighboring LF bins. This is equivalent to imposing a $\Delta\chi^2 = 1$ penalty when neighboring bins differ by 35%. Thus, if the data really demand a steep gradient, this penalty will permit one, but it will squash spurious gradients.

Figure 1 shows the resulting LF. This LF is significantly correlated with the completeness parameters (see eq. [10]), which are derived simultaneously,

$$f_{\rm break} = 43\% \pm 6\%\ , \qquad V_{\rm break} = 18.27 \pm 0.04\ . \tag{21}$$

In the Appendix, I consider arguments that might lead one to suspect that this estimate of $f_{\rm break}$ could be substantially too low. I find that these arguments are not compelling and therefore adopt the LF calculated using equation (21) as the best estimate. Nevertheless, in order to gain a sense of the possible role of such a systematic effect, I also show in Figure 1 the LF under the assumption that $f_{\rm break} = 65\%$, the highest value that I consider to be plausible.

Figure 2 compares the derived LF (with $f_{\rm break} = 43\%$) to those of several previous measurements of the halo LF: those of Bahcall & Casertano (1986), Dahn et al. (1995), and Gould et al. (1998), which were all previously compared by Gould et al. (1998). As explained there, the first two LFs are labeled "BC/CRB" and "DLHG/CRB" to indicate that they have been corrected from the originally published LFs to take account of the kinematic selection using the velocity ellipsoid of Casertano et al. (1990), which is very similar to the ellipsoid of Gould & Popowski (1998) and to the one derived for the present sample. The present measurement is in reasonably good agreement with the DLHG/CRB determination over the range $9 \le M_V \le 14$ covered by the latter. It disagrees strongly with both the BC/CRB and Gould et al. (1998) determinations (which are in good

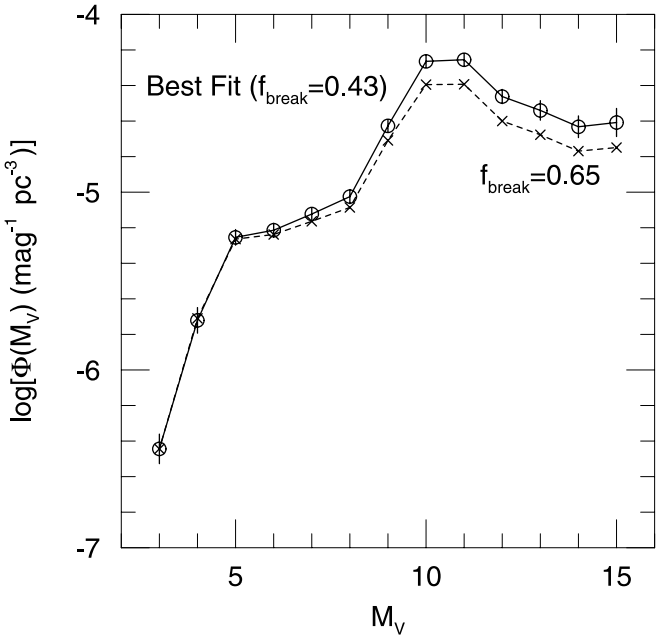

FIG. 1.—Logarithm of the LF derived from 4588 subdwarfs from the revised NLTT catalog (Gould & Salim 2003; Salim & Gould 2003). The solid curve and open symbols with error bars represent the best fit. The dashed curve and crosses represent the fit under the assumption that the derived catalog completeness has been seriously underestimated. The main features of the LF remain the same. The faintest two bins should be interpreted cautiously (see § 3.4).

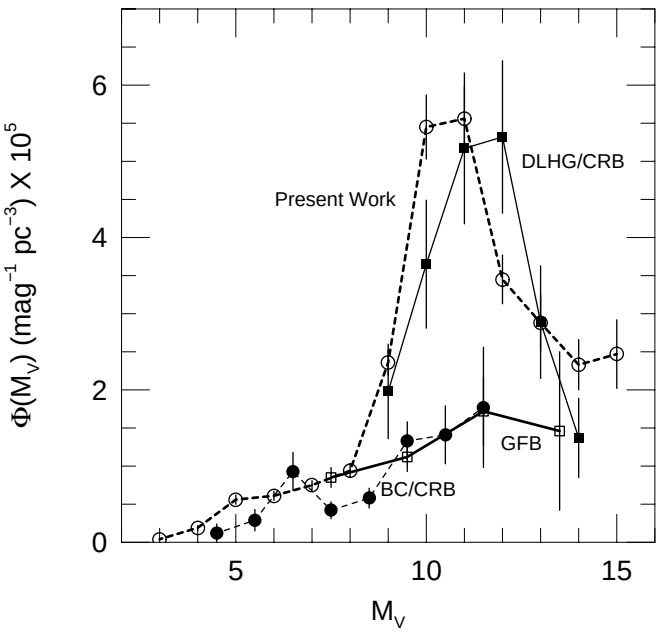

FIG. 2.—Comparison of four halo LFs. The original determinations by Dahn et al. (1995, DLHG) and Bahcall & Casertano (1986, BC) have been rescaled by Gould et al. (1998) using the velocity ellipsoid of Casertano et al. (1990, CRB). The present work confirms the "bump" in the LF found by DLHG at $M_V \sim 11$, as well as the fall-off toward brighter mags found by Bahcall & Casertano (1986) but with much smaller error bars in both cases.

agreement with each other). The new measurement extends over a much wider magnitude range and has substantially smaller error bars than any previous determination.

The LF evaluations at $M_V = 15$, and to a lesser extent at $M_V = 14$, should be interpreted cautiously because they depend sensitively on model assumptions. To understand this point, one should consider how ML "thinks" when fitting the LF. To zeroth order, it forms an LF in the naive way: by counting the number of stars whose dereddened observed $(V-J)_0$ color and the color-magnitude relation put them in a corresponding M_V bin, and dividing this number by the total effective volume probed by the survey for stars of that M_V. There are, respectively, 40 and 18 stars in the final two bins, but only roughly 20 and 6 of these are assigned to these bins by the final ML LF fit shown in Figures 1 and 2. What prevents ML from assigning much higher densities to the LF at these faint magnitudes? In the next brightest bin there are 159 stars. This is about 4 times larger than in the $M_V = 14$ bin despite the fact that the LF is roughly the same because the effective volume grows rapidly with luminosity at these faint magnitudes. As described above, ML takes this as a zeroth-order estimate for the number expected in this bin. It then considers how many of these are expected to scatter into neighboring bins because the color errors $\sigma(V-J) \simeq \sigma(V) = 0.25$ induce errors in M_V of $a\sigma(V) \sim 0.9$. That is, roughly 15% of these 159 stars are expected to scatter into the $M_V = 14$ bin and a few percent into the $M_V = 15$ bin. It is by accounting for this scatter, as well as scatter from brighter bins, that ML achieves its final estimate. This estimate therefore depends quite sensitively on the adopted value of $\sigma(V)$, which is described very simply in the model but could, in principle, actually be a function of V or of other variables.

In addition, because of the very small number of detected stars in these final bins, there is a potential problem of contamination from nonhalo stars. Contamination is not generally a problem because, as I argued in § 2.5, the discriminator η is limited to regions well away from main-sequence stars and white dwarfs. However, the density of the very dim halo stars on the RPM diagram is extremely low (see Salim & Gould 2003, Fig. 3), so even the low residual level of contamination could play a role.

To establish the LF at $M_V \geq 14$ more securely, and since the total number of stars in the last two bins is very small (58), the simplest approach would be to obtain V-band photometry for all of them. If the ML result is correct, the majority of these will be found to have scattered in from brighter bins. Metallicities and RVs from spectra of the truly red stars could then resolve issues of contamination. The LF of the final two bins would then rest on much firmer ground.

4. DISCUSSION

4.1. *Kinematics*

To high precision (roughly 2 km s^{-1}) the LSR is not moving with respect to the halo in either the radial or vertical directions. If the halo itself has no radial motion, the first result sharply contradicts the conclusion of Blitz & Spergel (1991) based on gas motions that the LSR is moving outward at 14 km s^{-1}. On the other hand, it is reasonably consistent with the radial-motion estimate of Metzger & Schechter (1994) based on carbon stars. More specifically, I find that the halo is moving at 11.4 ± 2.2 km s^{-1} relative to the Sun, and they find that the outer-Galaxy carbon stars are moving at 15.6 ± 1.7 km s^{-1}.

I find that all three off-diagonal components of the velocity dispersion tensor are small, within $\sim$2% of zero. The only previous measurements of these quantities (PG3) were consistent with zero but with errors that were about 4 times larger. To date, I am not aware of any effort to predict the off-diagonal terms from theory.

4.2. *Luminosity Function*

The measurement presented here of the LF confirms the basic peaked shape found by Dahn et al. (1995), but with about 40 times more stars and therefore covering a magnitude interval that is roughly twice as large. It is inconsistent with the flat LF found by Bahcall & Casertano (1986) and Gould et al. (1998; however, in principle, since the latter determination was based on stars away from the solar neighborhood, it cannot be rigorously ruled out by my measurement). The present measurement is in rough agreement with that of Bahcall & Casertano (1986) at brighter magnitudes, $M_V < 9$.

4.3. *Distance Scale*

A shortcoming of the present approach is that there is no information about distances within the data set, so the scale of the velocity ellipsoid must be set by external information. The distance scale could be set by obtaining either RVs or trigonometric parallaxes for a *representative* (i.e., random) subset of the stars in the sample. The former would yield a statistical parallax solution. I stress "representative" because if the subsample is biased—for example, is weighted toward stars with extreme kinematics and/or low metallicities—then the scale of the velocity ellipsoid will be overestimated by statistical parallax because the stars with RVs move faster than those in the sample as a whole. It would be misestimated by trigonometric parallax because the selected stars would be both faster and more subluminous than the sample as a whole. Hence, one must choose a fair sample and then make use of archival data only for stars within that sample.

From the standpoint of maximizing the precision of the distance-scale measurement with the minimum effort, statistical parallax is to be much preferred over trigonometric parallax. Even velocity errors of $\sim$20 km s^{-1} are quite adequate for a statistical parallax measurement with the limiting precision $\sigma(\eta)/\eta = 0.65N^{-1/2}$ (Popowski & Gould 1998a). Here N is the number of stars in the statistical parallax sample and η is the distance-scale parameter. Even assuming perfect parallaxes, the limit for the trigonometric parallax technique is $\sigma(\eta)/\eta = 0.2 \ln 10 \sigma(M_V) N^{-1/2}$. Given the large number of halo stars in the revised NLTT catalog and the relative ease of making RV compared to trigonometric parallax measurements, the modest per-star advantage of trigonometric parallax will be overwhelmed by the mass-production techniques available for RVs. However, good trigonometric parallaxes would provide information on the luminosity of individual stars, which cannot be obtained from statistical parallax techniques. Thus, the two approaches are complementary.

4.4. *Comparison with Parallax Data*

Parallaxes are currently available for a small subset of the *Luyten Half-Second* (LHS) catalog (Luyten 1979b), which is itself a subset of NLTT. LHS is reasonably complete for $\mu > 500$ mas yr^{-1} (see the Appendix) and contains a number of stars somewhat below this nominal limit. Monet et al. (1992) measure parallaxes for 69 LHS stars, and Gizis (1997) assembles parallaxes from various sources for an additional 60. Of these 129 stars, 70 are cross-identified in the revised NLTT catalog, of which 63 have *J*-band data from 2MASS. Figure 3 is an RPM diagram and a color-magnitude diagram (CMD) for these 63 stars. (For these plots, I use the CCD *V* photometry available from Monet et al. 1992 and Gizis 1997 in place of the generally photographic photometry from the revised NLTT.) The RPM diagram also shows all 2037 LHS stars from the revised NLTT catalog that have 2MASS *J* data. From this diagram, it is clear that the parallax stars are not a representative sample of LHS. Moreover, since they are assembled from heterogeneous sources, it would be quite difficult to determine their selection function. Hence, the CMD cannot be used to make a rigorous measurement of the color-magnitude relation.

Nevertheless, it is possible to glean important information from the CMD. I first fit linear color-magnitude relations to each of two subsets of the data: $1 < \eta \leq 4.15$ (*open circles*), and $0 < \eta \leq 4.15$ (*open circles and squares*). In both cases, I remove the two stars with $V-J > 4.13$ since this condition is also effectively applied when obtaining the results in § 3. That is, the bottom of the last bin is $M_V = 15.5$, which, according to the derived color-magnitude relation (eq. [20]), corresponds to $(V-J)_0 = (M_V - b)/a = 4.13$. (These two stars are quite interesting, and I return to them below.) In each case, I add an intrinsic scatter $\sigma(M_V)$ in quadrature to the measurement errors to force $\chi^2/\mathrm{dof} = 1$, which I find to be $\sigma(M_V) = 0.63$ mag and $\sigma(M_V) = 0.67$ mag, respectively. The resulting fits are shown as solid lines in the CMD and can be compared to the relation (eq. [20]) derived from the ML analysis, which is shown as a dashed line.

The first sample ($1 < \eta \leq 4.15$) corresponds to the selection used in the ML analysis. Recall that the lower boundary of this range has been set conservatively in order to reject disk stars. The sample is thus biased toward subluminous stars, a bias that is taken into account in the ML analysis but not here. One might therefore expect the derived color-magnitude relation to *underestimate* the luminosities. The second sample ($0 < \eta \leq 4.15$) goes to the disk/halo boundary advocated by Salim & Gould (2003) and thus eliminates this potential bias but at the cost of possible contamination by disk stars. One might therefore expect the derived color-magnitude relation to *overestimate* the luminosities. In fact, both relations are extremely close to equation (20), differing by 0.3 and 1.2 σ, respectively. Indeed, the first sample's relation is so close that the two can hardly be distinguished on the plot.

I now turn to the two red stars that were excluded from the fits, LHS 1742a (*circle*) and LHS 1166 (*square*). The CMD shows that they are brighter than the extrapolation of the adopted color-magnitude relation by 1.2 and 3.1 mag, respectively. Hence, these two stars may indicate that the color-magnitude relation, which is roughly linear at brighter magnitudes, could be turning sharply redward at the faint end. However, the 1.2 mag deviation of LHS 1742a is less than 2 σ and therefore not in itself remarkable, while the discriminator of LHS 1166 is $\eta = 0.08$, meaning that it could plausibly be a disk star. Hence, I examine the available information for each more closely.

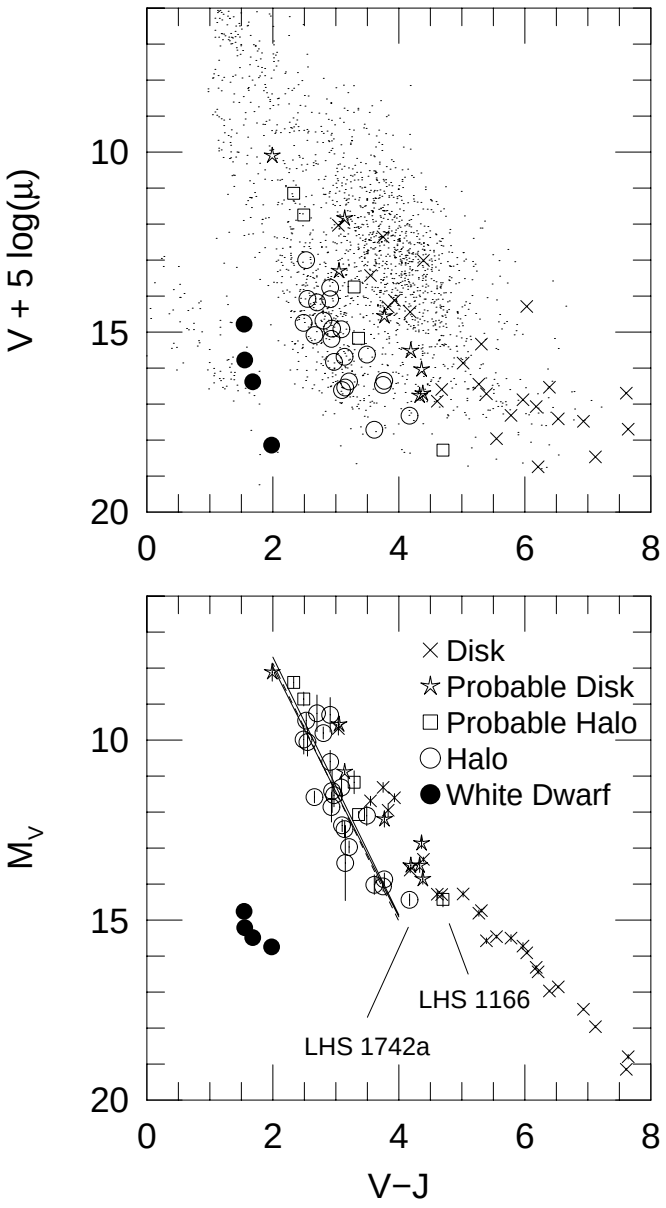

FIG. 3.—RPM diagram and CMD for 63 LHS stars with parallaxes and *J*-band data. Point types are by the discriminator η: crosses ($\eta \leq -1$, secure disk stars), stars ($-1 < \eta \leq 0$, probable disk stars), squares ($0 < \eta \leq 1$, probable halo stars), open circles ($1 < \eta \leq 4.15$, secure halo stars), and filled circles ($\eta > 6.15$, secure white dwarfs). (There are no stars in the white dwarf/halo boundary region, $4.15 < \eta \leq 6.15$.) The points in the RPM diagram show 2037 LHS stars with *J* data from the revised NLTT catalog. The dashed line in the CMD is the color-magnitude relation derived in § 3.3. The two solid lines are fits to the CMD halo stars either including (*upper line*) or excluding (*lower line*) those with $0 < \eta \leq 1$ (*squares*). These fits exclude the reddest two halo stars, LHS 1742a (*circle*) and LHS 1166 (*square*), whose CMD positions probably indicate that the color-magnitude relation bends toward the red at $V-J \sim 4$.

Gizis (1997) classifies LHS 1742a as esdM5.5, an extreme subdwarf; it lies in the extreme part of all three CaH/TiO5 diagrams. He assigns it a metallicity $[\mathrm{m/H}] = -2.0$. This star also has extreme kinematics: $(U, V, W) =$

$(-229, -263, 108)$ km s^{-1}. The intrinsic scatter $\sigma(M_V)$ derived above is due to differences in metallicity, with metal-weaker stars being fainter at fixed color (Gizis & Reid 1990). The fact that LHS 1742a is substantially brighter than the extension of the color-magnitude relation despite the fact that it is extremely metal-weak should therefore be regarded as evidence of a turn in that relation.

Unfortunately, a search of SIMBAD[1] reveals no new observations of LHS 1166 following the parallax measurement by Monet et al. (1992). This measurement showed that its transverse velocity is 224 ± 22 km s^{-1}, making the probability that it is a halo star very high. If so, the star's position on the CMD would show that the disk and halo color-magnitude relations either cross or merge at this point. Spectroscopic observations of this star to determine its spectral type, metallicity, and RV would help clarify this issue.

In brief, the linear color-magnitude relation adopted here is compatible with the parallax data for the colors $V-J < 4.13$ to which it is applied in the ML analysis of the revised NLTT catalog. However, there is evidence that the relation turns redward for later stars. While this evidence comes from only two stars and is incomplete for one of these, it nevertheless appears fairly convincing.

I thank Samir Salim for invaluable discussions about both the content and presentation of this paper. The comments and suggestions by the referee, John Gizis, improved the paper considerably. This work is supported by JPL contract 1226901 and by grant AST 02-01266 from the NSF.

[1] See http://simbad.u-strasbg.fr.

APPENDIX

COMPLETENESS

The principal source of systematic errors in this analysis is incompleteness (or rather, possible misestimation of the completeness) of the revised NLTT catalog. As shown in Figure 1, such misestimation can significantly affect the determination of the LF. However, I find that it does not affect the estimate of the velocity ellipsoid.

In principle, catalog completeness could be a function of all six observables, i.e., the V and J magnitudes, the proper motion, and the position on the sky. While the *relative completeness* of the revised NLTT compared to the original NLTT is very well understood (Salim & Gould 2003), there is substantially less information available about the *absolute completeness* of the underlying NLTT.

The completeness of NLTT can be tested either externally or internally. An external check requires an independent search for high proper-motion stars, either over the whole sky or some fraction of it. By comparing to the *Hipparcos* (ESA 1997) and Tycho-2 (Høg et al. 2000) catalogs, Gould & Salim (2003) concluded that NLTT is nearly 100% complete for $V \lesssim 11$ and for Galactic latitudes $|b| > 15°$. Even near to the plane, completeness is close to 100% for $\mu > 400$ mas yr^{-1}. Monet et al. (2000) searched for high proper-motion ($\mu > 400$ mas yr^{-1}) stars to faint magnitudes toward 1378 deg^2 and found 241 stars, only 17 of which (their Tables 2 and 3) they could not match to NLTT. In fact, two of these 17 are actually NLTT stars, namely, 58785 and 52890, which correspond to entries 1 and 8 from Table 3. Thus, over these surveyed areas, NLTT is $94\% \pm 2\%$ complete for $\mu > 400$ mas yr^{-1}. However, LHS (Luyten 1979b), a subset of NLTT that actually extends somewhat below 500 mas yr^{-1}, is almost certainly substantially more complete than is the NLTT at lower proper motions, so this measurement cannot be regarded as representative of NLTT as a whole.

Unfortunately, there are no systematic studies comparing NLTT detections with an independent search for proper-motion stars in the range 180 mas yr$^{-1} < \mu < 400$ mas yr^{-1} and at faint magnitudes. In the absence of such *external* checks, Flynn et al. (2001) conducted an *internal* completeness determination, whose approach is very closely related to the completeness measurement carried out here by ML. For a complete sample drawn from a stellar population that is uniformly distributed in space, the number of stars in the phase-space volume $[\mu_1,\ \mu_2] \times [V_1,\ V_2]$, should be (up to Poisson statistics) exactly 8 times the number in the volume $[2\mu_1,\ 2\mu_2] \times [V_1 - 5\log 2,\ V_2 - 5\log 2]$. This is because the former physical volume is 8 times larger, while the physical velocities being probed are exactly the same. Flynn et al. (2001) made a series of such comparisons at 0.5 mag intervals and, by multiplying these together, found that the completeness at $R_{\rm NLTT} = 18.5$ is 65% that at $R_{\rm NLTT} = 13$ (which latter they assumed to be 100%).

Monet et al. (2000) pointed out that *any* effect that reduced detections of more distant, slower moving stars (relative to faster nearby ones) could masquerade as incompleteness of fainter (relative to brighter) stars under this test. In particular, they argued that more distant stars would, being on average farther from the plane, have reduced density. Even a small difference of 4% in mean density per comparison could lead to the "observed" $f_{\rm break} = 65\%$ completeness at $R_{\rm NLTT,\,break} = 18.5$, since it would be multiplied together 11 times between $R_{\rm NLTT} = 13$ and 18.5. That is, $(1 - 0.04)^{11} \sim 65\%$. Monet et al. (2000) presented a figure showing that when the procedure is carried out on stars at lower Galactic latitude, the effect is much reduced.

This critique is important because the two-parameter characterization of incompleteness that I use here (see § 2.3) in essence embodies the Flynn et al. (2001) method. As noted in § 3.4, I find $f_{\rm break} = 43\% \pm 6\%$ at $V_{\rm break} = 18.27$. This fraction is consistent with the Flynn et al. (2001) result at the $1.5\,\sigma$ level when account is taken of the fact that I have assumed 100% completeness at $V = 12$ rather than $R_{\rm NLTT} = 13$. The magnitude $V_{\rm break}$ is slightly brighter than the value found by Flynn et al. (2001), but this is to be expected, since the revised NLTT catalog depends on 2MASS J-band cross identification.

However, the Monet et al. (2000) critique cannot account for the result found in equation (21) for several reasons. First, one does not expect the density of halo subdwarfs to fall off significantly within the volume probed by NLTT. Second, the ML fit actually allows for such a fall-off, so that even if the actual density did not satisfy this theoretical expectation, the fit would automatically take account of the fall-off. (In fact, according to eq. [19], the best fit is consistent with uniform density.) Third,

Flynn et al. (2001) are unable to reproduce Figure 3 from Monet et al. (2000) and instead find relatively comparable results when they apply their test to high-latitude and low-latitude stars.

Nonetheless, it remains possible that there is some *other* effect that reduces the counts of distant relative to nearby stars of the same class. One such effect would be incompleteness as a function of proper motion, rather than magnitude. Such incompleteness could be very pernicious because if the more distant (and hence slower moving) stars were under-represented by a mere 4%, then (as outlined above) the effect would be exponentiated and would generate a large apparent incompleteness as a function of magnitude. I therefore tested this hypothesis by including a proper-motion term for the completeness within the ML fit. However, this term did not improve the fit even slightly. One is thus left without any plausible explanation for the relative lack of more distant, slower stars, other than incompleteness as a function of magnitude.

The little direct information we have on the completeness of NLTT at faint magnitudes and relatively low proper motions is reasonably consistent with the ML estimates of completeness derived here. Reid (1990) searched for high proper-motion stars in a single Schmidt field toward the north Galactic pole. He recovered 63 stars from NLTT as well as 15 stars that met NLTT selection criteria but were not in NLTT. This appears to correspond to a mean completeness of 81%. However, three of the 15 have proper motions 180 mas $\mathrm{yr}^{-1} < \mu < 200$ mas yr^{-1}, i.e., within 1 σ (Salim & Gould 2003) of the NLTT limit. Stars that scatter across the selection boundary are *already* taken into account in the modeling procedure and should not be counted as due to "incompleteness." Hence, the true mean completeness of NLTT in the Reid (1990) survey area is more like $84\% \pm 5\%$. If one restricts consideration to stars $V < V_{\rm break}$ (beyond which the revised NLTT catalog is more sensitive to the incompleteness of 2MASS than NLTT), then $f_{\rm break} = 43\% \pm 6\%$ corresponds to a mean completeness of halo stars of $78\% \pm 3\%$, in 1 σ agreement with the value just derived from the Reid (1990) study.

In brief, there is no strong evidence to challenge the completeness estimate given by the ML fit.

REFERENCES

Backer, D. C., & Sramek, R. A. 1999, ApJ, 524, 805
Bahcall, J. N., & Casertano, S. 1986, ApJ, 308, 347
Blitz, L., & Spergel, D. N. 1991, ApJ, 370, 205
Casertano, S., Ratnatunga, K., & Bahcall, J. N. 1990, ApJ, 357, 435
Dahn, C. C., Liebert, J. W., Harris, H., & Guetter, H. C. 1995, in ESO Workshop on the Bottom of the Main Sequence and Beyond, ed. C. G. Tinney (Heidelberg: Springer), 239
Dehnen, W., & Binney, J. J. 1998, MNRAS, 298, 387
ESA. 1997, The *Hipparcos* and Tycho Catalogues (ESA SP-1200; Noordwijk: ESA)
Flynn, C., Sommer-Larsen, J., Fuchs, B., Graff, D. S., & Salim, S. 2001, MNRAS, 322, 553
Gizis, J. E. 1997, AJ, 113, 806
Gizis, J. E., & Reid, I. N. 1999, AJ, 117, 508
Gould, A. Bahcall, J. N., & Flynn, C. 1997, ApJ, 482, 913
Gould, A., Flynn, C., & Bahcall, J. N. 1998, ApJ, 503, 798
Gould, A., & Popowski, P. 1998, ApJ, 508, 844
Gould, A., & Salim, S. 2003, ApJ, 582, 1001
Høg, E., et al. 2000, A&A, 355, L27
Layden, A. C. 1994, AJ, 108, 1016
———. 1995, AJ, 110, 2288
———. 1997, PASP, 109, 524
Layden, A. C., Hanson, R. B., Hawley, S. L., Klemola, A. R., & Hanley, C. J. 1996, AJ, 112, 2110
Luyten, W. J. 1979a, New Luyten Catalogue of Stars with Proper Motions Larger than Two Tenths of an Arcsecond (Minneapolis: Univ. Minnesota Press)
Luyten, W. J. 1979b, A Catalogue of Stars with Proper Motions Exceeding 0″.5 Annually (Minneapolis: Univ. Minnesota Press)
———. 1980, New Luyten Catalogue of Stars with Proper Motions Larger than Two Tenths of an Arcsecond (Minneapolis: Univ. Minnesota Press)
Metzger, M. R., & Schechter, P. L. 1994, ApJ, 420, 177
Monet, D. G., Dahn, C. C., Vrba, F. J., Harris, H. C., Pier, J. R., Luginbuhl, C. B., & Ables, H. D. 1992, AJ, 103, 638
Monet, D. G., Fisher, M. D., Liebert, J., Canzian, B., Harris, H. C., & Reid, I. N. 2000, AJ, 120, 1541
Norris, J. 1986, ApJS, 61, 667
Oresme, N. 1377, Le Livre du Ciel et du Monde, MS Français 1082 (Paris: Bibliothèque Nationale)
Piotto, G., Cool, A. M., & King, I. R. 1997, AJ, 113, 1345
Popowski, P., & Gould, A. 1998a, ApJ, 506, 259
———. 1998b, ApJ, 506, 271
Reid, I. N. 1990, MNRAS, 247, 70
Reid, M. J., Readhead, A. C. S., Vermeulen, R. C., & Treuhaft, R. N. 1999, ApJ, 524, 816
Salim, S. & Gould, A. 2000, ApJ, 539, 241
———. 2002, ApJ, 575, L83
———. 2003, ApJ, 582, 1011
Siegel, M. H., Majewski, S. R., Reid, I. N., & Thompson, I. B. 2002, ApJ, 578, 151
Sommer-Larsen, J., & Zhen, C. 1990, MNRAS, 242, 10